Journal of the Korean Society for Nondestructive Testing
Vol. 25, No. 3 (2005. 6)

Application of a Modular Multi-Gaussian Beam Model to Ultrasonic Wave Propagation with Multiple Interfaces

Hyunjo Jeong*†, Moon-Cheol Park** and Lester W. Schmerr, Jr.***

Abstract A modular Gaussian beam model is developed to simulate some ultrasonic testing configurations where multiple interfaces are involved. A general formulation is given in a modular matrix form to represent the Gaussian beam propagation with multiple interfaces. The ultrasonic transducer fields are modeled by a multi-Gaussian beam model which is formed by superposing 10 single Gaussian beams. The proposed model, referred to as "MMGB" (modular multi-Gaussian beam) model, is then applied to a typical contact and angle beam testing configuration to predict the output signal reflected from the corner of a vertical crack. The resulting expressions given in a modular matrix form are implemented in a personal computer using the MATLAB program. Simulation results are presented and compared with available experimental results.

Keywords : Gaussian beam, modular form, multiple interface, transducer field, angle beam testing, crack corner reflection

1. Introduction

Modeling ultrasonic transducer fields is an important part when simulating a nondestructive evaluation (NDE) system. For this purpose, multi-Gaussian beam models (Song et al. 2004, Kim et al. 2004) have been used to describe the propagation of ultrasonic beams from piston transducers in many testing situations including multiple interfaces. As the number of interfaces increases, however, the analytical expressions for the amplitude and phase of a Gaussian beam become increasingly complex. Such cases can arise in practice, for example, when using angle beam shear waves (Kim et al. 2004). A modular Gaussian beam model (Schmerr and Sedov 2003) has been developed as an alternative approach. It provides an efficient formulation for ultrasound propagation because of its highly modular form after multiple interface interactions. The modular Gaussian approach was used to calculate the ultrasonic beams propagating through a multilayered isotropic medium with different interface curvatures (Huang et al. 2004).

In this paper, we briefly describe a highly modular multi-Gaussian beam model that can be efficiently used to simulate the propagation of ultrasonic beams in an isotropic solid with multiple interfaces. The model is then applied to predict the received voltage of corner reflection from a surface-breaking crack in a contact, angle beam testing configuration. Simulation results are presented for these problems and compared with available experimental results.

Received : February 17, 2005. Accepted : May 25, 2005. * Division of Mechanical and Automobile Engineering, Wonkwang University, Iksan, Korea, ** Korea Atomic Energy Research Institute, Daejon, Korea, *** Center for NDE and Department of Aerospace Engineering, Iowa State University, Ames, IA 50011, USA, † Corresponding author: hjjeong@wonkwang.ac.kr

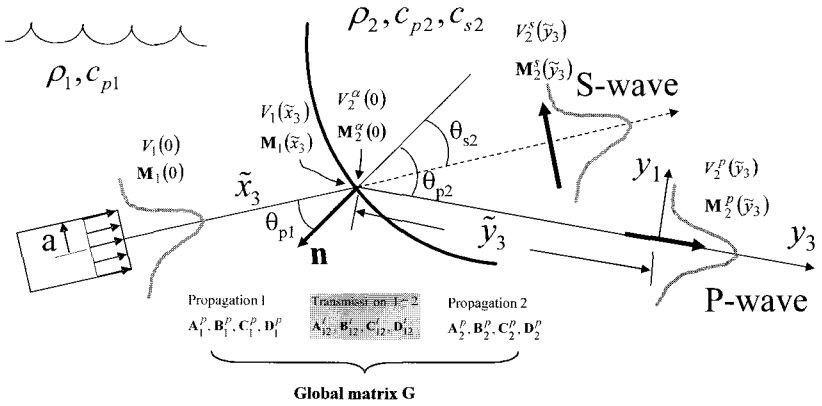

Fig. 1 A Gaussian beam propagation through a curved interface between a fluid and an isotropic solid. A modular Gaussian beam model can be formulated using the concept of global matrix composed of propagation matrices in medium 1 and 2, and transmission matrix from medium 1 to 2.

2. Modular multi-Gaussian beam model

We will describe the modular Gaussian approach for the immersion setup shown in Fig. 1 where a Gaussian beam is radiated at oblique incidence through a curved fluid-isotropic solid interface. For the geometry of Fig. 1, we will assume that a Gaussian velocity profile is present at the transducer and propagates as a Gaussian beam into the fluid. In Fig. 1, $V_1(0)$ and $\mathbf{M}_1(0)$ are the known starting amplitude and phase values in the Gaussian at the transducer location ($\tilde{x}_3 = 0$). The distances $\tilde{x}_3$ is taken as the propagation distances along the central axis of the Gaussian beam.

When the incident Gaussian beam strikes the curved fluid-solid interface, two refracted waves (compressional (P) and shear (S) waves) will be transmitted into the solid and one compressional wave will be reflected back into the fluid. In order to describe the transmitted waves in the solid we employ the coordinates $(y_1, y_2, \tilde{y}_3)$, taken along and perpendicular to the refracted waves. In the solid, $\tilde{y}_3$ is measured along the wave vector direction for a particular refracted wave type of $\alpha(\alpha = p$ or $s)$.

2.1. Propagation of a Gaussian beam - fluid, interface, and isotropic solid

The velocity amplitude $V_1(\tilde{x}_3)$ and phase $\mathbf{M}_1(\tilde{x}_3)$ of a propagating Gaussian beam in the fluid can be completely described by solving the paraxial wave equation (Huang 2004). When this Gaussian beam strikes a fluid-solid interface, reflected and transmitted Gaussian beams are generated. The amplitude $V_2^\alpha(0)$ and polarization vector $\overline{\mathbf{d}}^\alpha$ of the wave type α transmitted in the solid at the interface ($\tilde{y}_3 = 0$) in the paraxial approximation can be found by solving for the problem of the transmission of a plane wave at a planar interface. Thus, the refraction angles of transmitted waves in the solid can be determined by Snell's law, and the amplitude $V_2^\alpha(0)$ can be determined by multiplying the incident wave by the appropriate plane wave transmission coefficient. Obtaining the phase at the interface, $\mathbf{M}_2^\alpha(0)$, is more complicated. It involves matching the phases of the incident and transmitted waves at the

interface and approximating the interface surface to second order (if it is curved) (Schmerr and Sedov 2003) near the point where the central ray of the incident Gaussian strikes the interface. In the solid, the propagation laws for either a P- or S-wave (Gaussian amplitude and phase, $V_2^{\alpha}(\tilde{y}_3)$ and $M_2^{\alpha}(\tilde{y}_3)$) follow the same law as in the fluid.

2.2. A Modular Gaussian beam model

If we combine all of our previous results, it is possible to express the Gaussian beam in a modular matrix form by writing terms such as $\mathbf{M}_2^{\alpha}(\tilde{y}_3)$ directly in terms of the known $\mathbf{M}_1(0)$ by introducing global matrices $(\mathbf{A}^G, \mathbf{B}^G, \mathbf{C}^G, \mathbf{D}^G)$ where

$$\mathbf{G} = \begin{bmatrix} \mathbf{A}^G & \mathbf{B}^G \\ \mathbf{C}^G & \mathbf{D}^G \end{bmatrix} = \begin{bmatrix} \mathbf{A}_2^p & \mathbf{B}_2^p \\ \mathbf{C}_2^p & \mathbf{D}_2^p \end{bmatrix} \begin{bmatrix} \mathbf{A}_{12}^t & \mathbf{B}_{12}^t \\ \mathbf{C}_{12}^t & \mathbf{D}_{12}^t \end{bmatrix} \begin{bmatrix} \mathbf{A}_1^p & \mathbf{B}_1^p \\ \mathbf{C}_1^p & \mathbf{D}_1^p \end{bmatrix} \tag{1}$$

In terms of global matrices, one can show that (Huang 2004)

$$V_2^{\alpha}(\tilde{y}_3) = \frac{V_1(0) T_{12}^{\alpha;p} \sqrt{\det[\mathbf{A}_{12}^t]}}{\sqrt{\det[\mathbf{A}^G + \mathbf{B}^G \mathbf{M}_1^0]}} = \sqrt{\frac{\rho_1 c_{p1}}{\rho_2 c_{\alpha 2}}} \frac{V_1(0) \bar{T}_{12}^{\alpha;p}}{\sqrt{\det[\mathbf{A}^G + \mathbf{B}^G \mathbf{M}_1(0)]}} \tag{2}$$

$$\mathbf{M}_2^{\alpha}(\tilde{y}_3) = [\mathbf{D}^G \mathbf{M}_1(0) + \mathbf{C}^G][\mathbf{B}^G \mathbf{M}_1(0) + \mathbf{A}^G]^{-1} \tag{3}$$

where $\bar{T}_{12}^{\alpha;\beta} = T_{12}^{\alpha;\beta} \sqrt{\frac{\rho_2 c_{\alpha 2} \cos\theta_{\alpha 2}}{\rho_1 c_{\beta 1} \cos\theta_{\beta 1}}}$ is the normalized transmission coefficient for an incident wave of type β and a transmitted wave of type α. Here, $T_{12}^{\alpha;\beta}$ is the usual transmission coefficient based on the particle velocity ratio (Rudolph 1999). Similar expressions can be obtained for the interface reflection, although not shown here. In Eq. (3), $\mathbf{M}_1(0) = \frac{1}{c_{p1}}\left(\frac{1}{R_0} + i\frac{2}{k_{p1} w_0^2}\right)\mathbf{I}$, where R_0 and w_0 are radius of curvature and width of the Gaussian profile in the plane of transducer face, c_{p1} and k_{p1} the wave speed and the wave number in the fluid, and I a 2x2 identity matrix.

In Eq. (1), the propagation matrices $(\mathbf{A}_1^p, \mathbf{B}_1^p, \mathbf{C}_1^p, \mathbf{D}_1^p)$ in the fluid are given by

$$\mathbf{A}_1^P = \mathbf{D}_1^p = \begin{bmatrix} 1 & 0 \\ 0 & 1 \end{bmatrix}, \quad \mathbf{B}_1^P = c_{p1} \tilde{x}_3 \begin{bmatrix} 1 & 0 \\ 0 & 1 \end{bmatrix}, \quad \mathbf{C}_1^P = \begin{bmatrix} 0 & 0 \\ 0 & 0 \end{bmatrix} \tag{4}$$

For a fluid/isotropic solid interface the transmission matrices in Eq. (1) $(\mathbf{A}_{12}^t, \mathbf{B}_{12}^t, \mathbf{C}_{12}^t, \mathbf{D}_{12}^t)$ are given by

$$A_{12}^t = \begin{bmatrix} \frac{\cos\theta_{\alpha 2}}{\cos\theta_{p1}} & 0 \\ 0 & 1 \end{bmatrix}, \quad B_{12}^t = \begin{bmatrix} 0 & 0 \\ 0 & 0 \end{bmatrix},$$
$$C_{12}^t = \left(\frac{\cos\theta_{p1}}{c_{p1}} - \frac{\cos\theta_{\alpha 2}}{c_{\alpha 2}}\right) \begin{bmatrix} \frac{h_{11}}{\cos\theta_{p1}\cos\theta_{\alpha 2}} & \frac{h_{12}}{\cos\theta_{\alpha 2}} \\ \frac{h_{21}}{\cos\theta_{p1}} & h_{22} \end{bmatrix}, \tag{5}$$
$$D_{12}^t = \begin{bmatrix} \frac{\cos\theta_{p1}}{\cos\theta_{\alpha 2}} & 0 \\ 0 & 1 \end{bmatrix}$$

Similarly, the propagation matrices $(\mathbf{A}_2^p, \mathbf{B}_2^p, \mathbf{C}_2^p, \mathbf{D}_2^p)$ in the solid are

$$\mathbf{A}_2^P = \mathbf{D}_2^p = \begin{bmatrix} 1 & 0 \\ 0 & 1 \end{bmatrix}, \quad \mathbf{B}_2^P = c_{\alpha 2} \tilde{y}_3 \begin{bmatrix} 1 & 0 \\ 0 & 1 \end{bmatrix}, \quad \mathbf{C}_2^P = \begin{bmatrix} 0 & 0 \\ 0 & 0 \end{bmatrix} \tag{6}$$

In Eqs. (3)-(5), c_{p1} is the P-wave velocity in the fluid, while $c_{\alpha 2}$ is the velocity for a wave of type α in the solid. $(h_{11}, h_{12} = h_{21}, h_{22})$ are the curvatures of the interface in and perpendicular to the plane of incidence.

2.3. Propagation through multiple interfaces

The modular way of expressing the Gaussian beam propagation can be conveniently generalized for the case of N transmissions or

reflections. In this case, the velocity of the Gaussian beam at a point $\hat{\mathbf{Y}} = (y_1, y_2, \tilde{y}_3)$ in the Nth medium can be written as

$$\mathbf{v}^{\alpha}(\hat{\mathbf{Y}},\omega) = \sqrt{\frac{\rho_1 c_{p1}}{\rho_{N+1} c_{\alpha(N+1)}}} \frac{V_1(0)\,\bar{\mathbf{d}}^{\alpha} \prod_{m=1}^{N} \bar{T}^{\alpha;\beta}_{m\,m+1}}{\sqrt{\det\left[\mathbf{A}^G + \mathbf{B}^G\,\mathbf{M}_1(0)\right]}} \times \exp\left[i\omega \left(\sum_{m=1}^{N+1} \frac{x_m}{c_{\alpha m}} + \frac{1}{2}\mathbf{Y}^T \mathbf{M}^{\alpha}_{N+1}(\tilde{y}_3)\mathbf{Y} \right) \right]$$

$$\mathbf{Y} = [y_1 \quad y_2]^T \tag{7}$$

where $\bar{T}^{\alpha;\beta}_{m\,m+1}$ is the normalized appropriate transmission coefficient for the mth interface and $c_{\alpha m}$ is the magnitude of the phase velocity for the appropriate wave in the mth medium. In this case we also have

$$\mathbf{M}^{\alpha}_{N+1}(\tilde{y}_3) = \left[\mathbf{D}^G\,\mathbf{M}_1(0) + \mathbf{C}^G\right]\left[\mathbf{B}^G\,\mathbf{M}_1(0) + \mathbf{A}^G\right]^{-1} \tag{8}$$

where

$$\mathbf{G} = \begin{bmatrix} \mathbf{A}^G & \mathbf{B}^G \\ \mathbf{C}^G & \mathbf{D}^G \end{bmatrix} = \begin{bmatrix} \mathbf{A}^P_{N+1} & \mathbf{B}^P_{N+1} \\ \mathbf{C}^P_{N+1} & \mathbf{D}^P_{N+1} \end{bmatrix} \cdots \begin{bmatrix} \mathbf{A}^I_{12} & \mathbf{B}^I_{12} \\ \mathbf{C}^I_{12} & \mathbf{D}^I_{12} \end{bmatrix} \begin{bmatrix} \mathbf{A}^P_1 & \mathbf{B}^P_1 \\ \mathbf{C}^P_1 & \mathbf{D}^P_1 \end{bmatrix} \tag{9}$$

2.4. Modular multi-Gaussian beam model

Using the approach of Wen and Breazeale (Wen and Breazeale 1988), by the superposition of 10 Gaussian beams, one can model the corresponding wave field of a circular piston source (of radius a). In this manner, Eq. (7) can be written as

$$\mathbf{v}^{\alpha}(\omega) = \sqrt{\frac{\rho_1 c_{p1}}{\rho_{N+1} c_{\alpha(N+1)}}} \sum_{n=1}^{10} \frac{V_1(0)\,A_n\,\bar{\mathbf{d}}^{\alpha} \prod_{m=1}^{N} \bar{T}^{\alpha;\beta}_{m\,m+1}}{\sqrt{\det\left[\mathbf{A}^G + \mathbf{B}^G\,(\mathbf{M}_1(0))_n\right]}} \times \exp\left[i\omega \left(\sum_{m=1}^{N+1} \frac{x_m}{c_{\alpha m}} + \frac{1}{2}\mathbf{Y}^T \mathbf{M}^{\alpha}_{N+1}(\tilde{y})\mathbf{Y} \right) \right] \tag{10}$$

where $(\mathbf{M}_1(0))_n = \dfrac{2\,i\,B_n}{\omega\,a^2}\mathbf{I}$, and A_n and B_n are ten complex constants (Wen and Breazeale 1988). Eq. (10) provides a highly efficient formulation for modeling the wave fields of ultrasonic transducers in very complex testing situations, and will be referred to as the "MMGB" model.

3. Simulation of reflection from the corner of a vertical crack

We have described a highly modular multi-Gaussian beam (MMGB) approach for the immersion setup shown in Fig. 1. The modular model, however, is also directly applicable to a variety of contact and angle-beam testings as well. We consider a typical contact, angle beam testing as shown in Fig. 2. The specimen used in this study is a steel plate of 10 mm height and 25.4 mm width (w_c). The depth (h_c) of a surface breaking crack is 2 mm. For the angle beam testing, a longitudinal wave transducer (5 MHz center frequency and 9.5 mm diameter) is mounted on a Lucite wedge to generate a 45° refracted shear wave into the specimen. The distance of central beam path within the wedge is 10 mm.

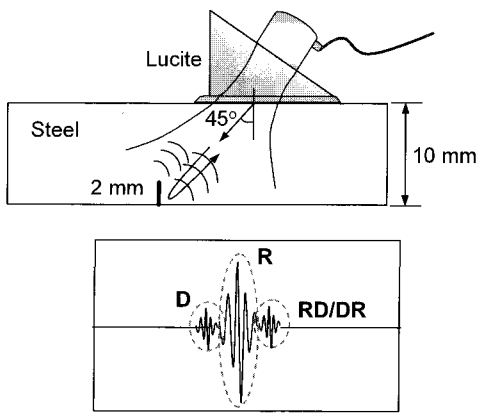

Fig. 2 Illustration of a contact, angle beam ultrasonic testing for a surface breaking crack and typical waveforms of received signal.

The received signals for this configuration are typically composed of three parts due to: (1) crack tip diffraction (denoted by "D"), (2) reflection from around the crack corner (denoted by "R"), and (3) reflection from the bottom of

the specimen and then crack-tip diffraction plus diffraction from the tip and then reflection from the bottom (denoted by "RD/DR").

We apply the MMGB model to predict the second part of the received signal only. When the axis of the central beam aims at the crack corner, the upper half of the incident beam will hit the crack face first and then reflected from the bottom surface of the specimen. The lower half of the incident beam will impinge on the bottom surface first and then reflected from the crack face. Consequently, these two beams will experience the same travel path and transmissions/reflections. So the total beam will normally strike the crack height of 2 h_c as shown in Fig. 3.

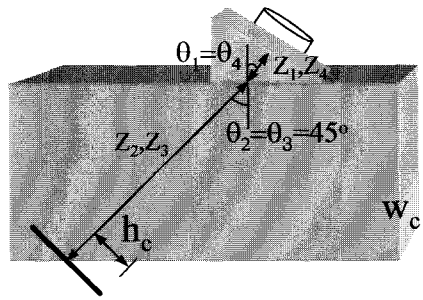

Fig. 3 A schematic representation of angle beam ultrasonic testing to calculate the received signal due to reflection from the crack corner when the axis of central beam aims at the crack corner.

The received voltage due to the reflection from the crack corner can be calculated by taking the average velocity of $v(\omega)$ over the transducer face S_T multiplied by the system efficiency factor $\beta(\omega)$ (Schmerr 1998):

$$V(\omega)=\frac{\beta(\omega)}{S_T}\int_{S_T} v(\omega)\,dS \tag{11}$$

where $v(\omega)$ is the particle velocity at the receiving transducer face given by

$$v(\omega)=\int_{w_c}\int_{2h_c}\sum_{n=1}^{10}\frac{A_n\,T_{12}^{s;p}\,T_{21}^{p;s}\,(R_{23}^{s;s})^2}{\sqrt{\det\left[\mathbf{A}^G+\mathbf{B}^G\,(\mathbf{M}_1(0))_n\right]}} \exp\left[i\omega\left(\frac{2z_1}{c_{p1}}+\frac{2z_2}{c_{s2}}+\frac{1}{2}\,\mathbf{Y}^T\mathbf{M}_4^p(z_1)\mathbf{Y}\right)\right]dh\,dw \tag{12}$$

and

$$\mathbf{M}_4^p(z_1)=\left[\mathbf{D}^G\,\mathbf{M}_1(0)+\mathbf{C}^G\right]\left[\mathbf{B}^G\,\mathbf{M}_1(0)+\mathbf{A}^G\right]^{-1} \tag{13}$$

The reflection coefficient $R_{23}^{s;s}$ in Eq. (12) is calculated for the 45° shear wave incidence. The system efficiency factor $\beta(\omega)$ will be discussed later. The global matrices in the Gaussian phase in Eq. (13) are given by

$$\begin{bmatrix}\mathbf{A}^G & \mathbf{B}^G\\ \mathbf{C}^G & \mathbf{D}^G\end{bmatrix}=\begin{bmatrix}\mathbf{A}_4^p & \mathbf{B}_4^p\\ \mathbf{C}_4^p & \mathbf{D}_4^p\end{bmatrix}\begin{bmatrix}\mathbf{A}_{34}^t & \mathbf{B}_{34}^t\\ \mathbf{C}_{34}^t & \mathbf{D}_{34}^t\end{bmatrix}\begin{bmatrix}\mathbf{A}_3^p & \mathbf{B}_3^p\\ \mathbf{C}_3^p & \mathbf{D}_3^p\end{bmatrix} \times\begin{bmatrix}\mathbf{A}_{23}^r & \mathbf{B}_{23}^r\\ \mathbf{C}_{23}^r & \mathbf{D}_{23}^r\end{bmatrix}\begin{bmatrix}\mathbf{A}_2^p & \mathbf{B}_2^p\\ \mathbf{C}_2^p & \mathbf{D}_2^p\end{bmatrix}\begin{bmatrix}\mathbf{A}_{12}^t & \mathbf{B}_{12}^t\\ \mathbf{C}_{12}^t & \mathbf{D}_{12}^t\end{bmatrix}\begin{bmatrix}\mathbf{A}_1^p & \mathbf{B}_1^p\\ \mathbf{C}_1^p & \mathbf{D}_1^p\end{bmatrix} \tag{14}$$

For propagation and transmissions/reflection matrices in Eq. (14), we have

$$\mathbf{A}_1^p=\mathbf{A}_4^p=\begin{bmatrix}1 & 0\\ 0 & 1\end{bmatrix}\quad \mathbf{B}_1^p=\mathbf{B}_4^p=c_1 z_1\begin{bmatrix}1 & 0\\ 0 & 1\end{bmatrix}$$

$$\mathbf{C}_1^p=\mathbf{C}_4^p=\begin{bmatrix}0 & 0\\ 0 & 0\end{bmatrix}\quad \mathbf{D}_1^p=\mathbf{D}_4^p=\begin{bmatrix}1 & 0\\ 0 & 1\end{bmatrix}$$

$$\mathbf{A}_{12}^t=\begin{bmatrix}\frac{\cos\theta_2}{\cos\theta_1} & 0\\ 0 & 1\end{bmatrix}\quad \mathbf{B}_{12}^t=\begin{bmatrix}0 & 0\\ 0 & 0\end{bmatrix}$$

$$\mathbf{C}_{12}^t=\left(\frac{\cos\theta_1}{c_1}-\frac{\cos\theta_2}{c_2}\right)\begin{bmatrix}0 & 0\\ 0 & 0\end{bmatrix}\quad \mathbf{D}_{12}^t=\begin{bmatrix}\frac{\cos\theta_1}{\cos\theta_2} & 0\\ 0 & 1\end{bmatrix}$$

$$\mathbf{A}_2^p=\mathbf{A}_3^p=\begin{bmatrix}1 & 0\\ 0 & 1\end{bmatrix}\quad \mathbf{B}_2^p=\mathbf{B}_3^p=c_2 z_2\begin{bmatrix}1 & 0\\ 0 & 1\end{bmatrix}$$

$$\mathbf{C}_2^p=\mathbf{C}_3^p=\begin{bmatrix}0 & 0\\ 0 & 0\end{bmatrix}\quad \mathbf{D}_2^p=\mathbf{D}_3^p=\begin{bmatrix}1 & 0\\ 0 & 1\end{bmatrix}$$

$$\mathbf{A}_{23}^r=\begin{bmatrix}-\frac{\cos\theta_3}{\cos\theta_2} & 0\\ 0 & 1\end{bmatrix}\quad \mathbf{B}_{23}^r=\begin{bmatrix}0 & 0\\ 0 & 0\end{bmatrix}$$

$$\mathbf{C}_{23}^r=\left(\frac{\cos\theta_2}{c_2}+\frac{\cos\theta_3}{c_3}\right)\begin{bmatrix}0 & 0\\ 0 & 0\end{bmatrix}\quad \mathbf{D}_{23}^r=\begin{bmatrix}-\frac{\cos\theta_2}{\cos\theta_3} & 0\\ 0 & 1\end{bmatrix}$$

$$\mathbf{A}_{34}^t=\begin{bmatrix}\frac{\cos\theta_1}{\cos\theta_2} & 0\\ 0 & 1\end{bmatrix}\quad \mathbf{B}_{34}^t=\begin{bmatrix}0 & 0\\ 0 & 0\end{bmatrix}$$

$$\mathbf{C}_{34}^t=\left(\frac{\cos\theta_2}{c_2}-\frac{\cos\theta_1}{c_1}\right)\begin{bmatrix}0 & 0\\ 0 & 0\end{bmatrix}\quad \mathbf{D}_{34}^t=\begin{bmatrix}\frac{\cos\theta_2}{\cos\theta_1} & 0\\ 0 & 1\end{bmatrix}$$

where $c_1 = c_4 = 2680\,\text{m/s}$, $c_2 = c_3 = 3240\,\text{m/s}$, $\theta_1 = \theta_4 = 35.8°$, $\theta_2 = \theta_3 = 45°$.

4. System efficiency factor

In an actual ultrasonic experiment, the quantity that is usually measured is a voltage versus time, $V_O(t)$. If this voltage signal is digitized and Fourier transformed, we will have the voltage versus frequency, $V_O(\omega)$. For a linear ultrasonic system, it is assumed that $V_O(\omega)$ is proportional to the average velocity received by a transducer. The average velocity is provided by a model, as shown previously.

In the measurement of an output voltage from a flaw, for instance, there are involved a number of physical processes such as pulser/receiver, cables, piezoelectric effect of transducer, material attenuation, propagation, transmission/reflection, diffraction, and flaw scattering. Among these elements, the parameters associated with the piezoelectric effect, pulser/receiver and cables are difficult to model, although not impossible (Dang and Schmerr 2001). We can avoid this difficulty by grouping all these hard-to-model terms into a single parameter which is called the system efficiency factor, $\beta(\omega)$. With the aid of $\beta(\omega)$ the direct comparison can be made between model prediction and experiment.

The system efficiency factor can be determined by the deconvolution of an experimental signal $[V_O(\omega)]$ captured for the reference reflector by the model-predicted signal $[V_R(\omega)]$ for the same configuration. Since, as is well known, such deconvolution is sensitive to noise, it is usually performed with the aid of a Wiener filter $W(\omega)$, i.e.

$$\beta(\omega) = \frac{V_O(\omega)}{V_R(\omega)} W(\omega) \tag{15}$$

In this study, it is decided to use the circular part of the STB-A1 block (Fig. 4) as a reference reflector. This reflector was also used by Kim and Song (2002). Fig. 5(a) shows the experimental signal captured from the circular part of the STB-A1 block with a 5 MHz, 9.5 mm diameter transducer. By the deconvolution of this signal by the model-based reference reflector signal we can determine the system efficiency factor as shown in Fig. 5(b).

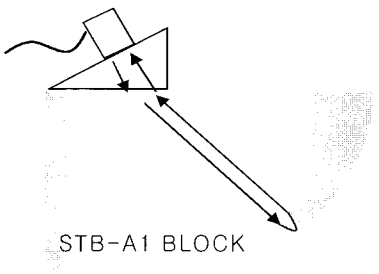

Fig. 4 STB-A1 block used as a reference reflector for determining the system efficiency factor $\beta(\omega)$.

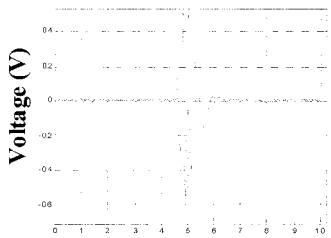

(a)

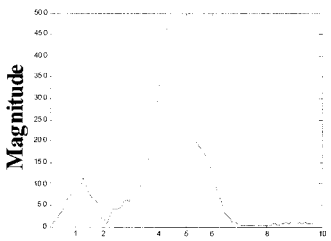

(b)

Fig. 5 (a) An experimental reference signal acquired from the circular part of the STB-A1 block, and (b) the calculated system efficiency factor.

5. Model prediction and comparison with experiment

In order to calculate the MMGB model prediction, the resulting expression given in Eq. 11 was implemented in a personal computer using the MATLAB program. Fig. 6(a) shows the calculated waveforms when the axis of central beam aims at the crack corner. The present model only predicts the signal reflected from the crack corner, so it does not present the first and third parts of signal usually observed in an angle beam testing with crack present (These signals are schematically illustrated in Fig. 2).

It is important to verify the proposed MMGB model by experiments for further applications of the model in many practical NDE problems. The experiment was also conducted for the current problem with the same equipment settings as in the reference reflector experiment. The experimental measurements are shown in Fig. 6(b). Comparisons of Figs. 6(a) and 6(b) exhibit a good agreement in terms of amplitude and waveform shape. The experimental signal also shows the signal groups diffracted from the crack tip. The relatively good agreement demonstrates the high accuracy of the developed model for simulating the multiple propagation and transmissions/reflections problem. The good agreement observed in this investigation suggests that the proposed MMG model can be used for simulating the multiple propagation and transmissions/reflections problems with high accuracy.

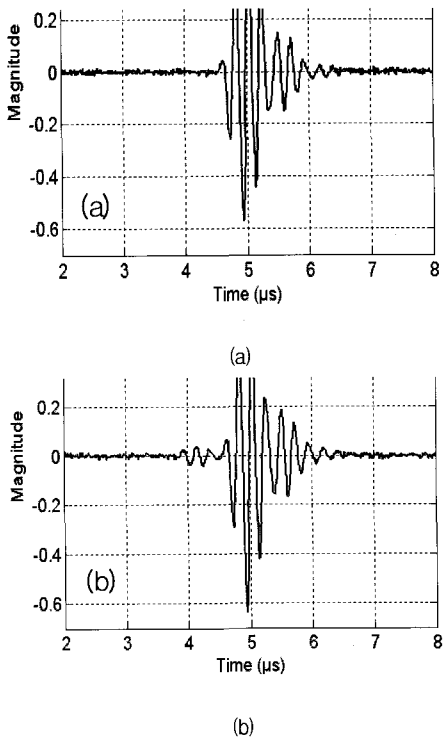

Fig. 6 Comparison of the MMGB model prediction (a) and the experiment (b) when the axis of central beam aims at the crack corner.

6. Conclusion

We have described a highly modular multi-Gaussian beam (MMGB) model that can be efficiently used to simulate the propagation of ultrasonic fields in an isotropic solid with multiple interfaces. The model was applied to a contact, angle beam testing for a surface breaking crack where multiple propagation and transmissions are involved. Model prediction was made to predict the crack corner reflection signal when the axis of the central beam aims at the crack corner. The model prediction agreed well with the experiment. The good agreement observed in this investigation suggests that the proposed MMG model can be used for simulating the multiple propagation and transmissions/reflections problems with high accuracy. The proposed MMGB model can be extended to the case of anisotropic materials with multiple interfaces.

Acknowledgement

This work was supported by the grant number R05-2004-000-10979-0 of the Korea Science and Engineering Foundation (KOSEF).

References

Dang, C. and Schmerr, L. W. (2001) Complete modeling of an ultrasonic NDE measurement system - an electroacoustic measurement model, *J. Kor. Soc. Nondestr. Testing,* 21, pp. 1-21

Huang, R., Schmerr, L. W. and Sedov, A., (2004) Modeling ultrasonic fields of a transducer with a modular multi-Gaussian beam model, *Rev. Prog. Quant. Nondestr. Eval.,* 23, pp. 745-752

Kim, H.-J. and Song, S.-J. (2002) Prediction of angle beam ultrasonic testing signals using multi-Gaussian beams, *Rev. Prog. Quant. Nondestr. Eval.,* 21, pp. 839-846

Kim, H.-J. and Song, S.-J. and Schmerr, L. W. (2004) Modeling ultrasonic pulse-echo signals from a flat-bottom hole in immersion testing using a multi-Gaussian beam, *J. NDE,* 23, pp. 11-19

Rudolph, M. (1999) *Ultrasonic beam models in anisotropic media,* Ph.D. Thesis, Iowa State University

Schmerr, L. W. (1998) *Fundamentals of ltrasonic Nondestructive Evaluation: A Modeling a Approach*, Plenum, New York

Schmerr, L. W. and Sedov, A. (2003) A modular multi-Gaussian beam model for isotropic and anisotropic media, *Rev. Prog. Quant. Nondestr. Eval.,* 22, pp. 828-835

Song, S.-J., Park, J.-S., Kim, Y. H., Jeong, H. and Choi, Y.-H. (2004) Prediction of angle beam ultrasonic testing signals from a surface breaking crack in a plate using multi-Gaussian beams and ray methods, *Rev. Prog. Quant. Nondestr. Eval.,* 23, pp. 110-117

Wen, J. J. and Breazeale, M. A. (1988) A diffraction beam field expressed as the superposition of Gaussian beams, *J. Acoust. Soc. Am.,* 83, pp. 1752-1756